Mon. Not. R. Astron. Soc. **000**, 1–?? (2004) Printed 7 August 2009 (MN LaTeX style file v2.2)

The beam topology and dynamic emission properties of pulsar B0943+10 — VI. Discovery of a 'Q'-mode precursor and comparison with pulsar B1822–09

Isaac Backus[1], Dipanjan Mitra[2] & Joanna M. Rankin[3,1]
[1]*Physics Department, University of Vermont, Burlington, VT 05405 USA*⋆
[2]*National Centre for Radio Astrophysics, Ganeshkhind, Pune 411 007 India*†
[3]*Sterrenkundig Instituut 'Anton Pannekoek', University of Amsterdam, NL-1098 SJ*

Unreleased

ABSTRACT

This paper reports new observations of pulsars B0943+10 and B1822–09 carried out with the Arecibo Observatory (AO) and Giant Metrewave Radio Telescope (GMRT), respectively. Both stars exhibit two modes. We report the discovery in B0943+10 of a highly linearly polarized "precursor" component that occurs significantly in only one mode. This emission feature closely resembles B1822–09's precursor which also occurs brightly in only one mode. B0943+10's other mode is well known for its highly regular drifting subpulses that are apparently produced by a rotating "carousel" system of 20 'beamlets.' Similary, B1822–09 exhibits subpulse-modulation behavior only in the mode where its precursor is absent. We survey our 18 hours of B0943+10 observations and find that the 'sideband'-modulation features, from which the carousel-rotation time can be directly determined, occur very rarely—less that 5% of the time—but always indicating 20 'beamlets'. We then present an analysis of B1822–09's modal modulation characteristics at 325-MHz and compare them in detail with B0943+10. The pulsar never seems to null, and we find a 43-rotation-period P_3 feature in the star's 'Q' mode that modulates the interpulse as well as the conal feature s in the main pulse. We conclude that B1822–09 must have a nearly orthogonal geometry and that its carousel circulation time is long compared to the modal subsequences available in our observations. Finally, we find that the mainpulse/interpulse separation is almost exactly 180°, and we assess the interesting suggestion by Dyks *et al* that downward-going radiation produces B1822–09's precursor emission.

Key words: MHD, plasmas, pulsars: radiation mechanism, polarization, mode-changing phenomenon, precursor, interpulse – B0943+10, B1822–09

I. INTRODUCTION

Among the well investigated pulsars that exhibit the phenomenon of "mode switching", B0943+10 provides one of the clearest examples of two discrete modes, both exhibiting distinct, fully characterizable behaviors (Suleymanova & Izvekova 1984). In this paper, the sixth in a series describing B0943+10 analyses, we (somewhat abashedly) report a newly discovered 'Q'-mode precursor feature in the profile of this intriguing star, suggesting a strong similarity to another well studied pulsar with highly discrete modes, B1822–09 (or J1825–0935).

During its weak, 'Q'uiescent mode, the B0943+10 is well known to exhibit a chaotic subpulse-modulation behavior (Suleymanova *et al* 1988; hereafter SIRR). By constrast, its 'B'urst mode has been of great interest throughout this series, in that it now stands as the paradigm example of regularly drifting subpulses. Analysis has repeatedly shown that the observed 'B'-mode pattern of subpulses results from a rotating carousel of just 20 'beamlets,' such that consistent subbeam-carousel maps have been constructed for observations at a number of different epochs (Deshpande & Rankin 2001; Asgekar & Deshpande 2001; hereafter Paper I and Paper II of this series).

An important finding for developing a complete model of the polar cap emission region of B0943+10 was the presence of evenly spaced 'sidebands' surrounding the primary modulation feature associated with drifting subbeams. In

⋆ Isaac.Backus@uvm.edu; Joanna.Rankin@uvm.edu
† dmitra@ncra.tifr.res.in;

Table 1. B0943+10 and B1822–09 Observations

MJD	Frequency (MHz)	Resolution (°longitude)	Length (in pulses)
AO B0943+10			
[a]48914	430	0.330	986
[b]52709	327	0.352	6748
[b]52711	327	0.352	6809
52832	327	0.352	7559
52840	327	0.352	7275
52916	327	0.352	6560
52917	327	0.352	3024
53491	327	0.459	5841
53492	327	0.459	6825
53862	327	0.352	5041
54016	327	0.352	6012
54630	327	0.352	7569
54632	327	0.352	6656
GMRT B1822–09			
53780	325	0.240	[c]2077
[b]54864	325	0.240	2106

The files of the B0943+10 observations used in this analysis were resampled from their original resolution. Higher resolution is available, but was unnecessary for the analysis presented here.
[a]Only 41° are available for this observation
[b]This observation lacks polarimetry
[c]The original observation contains 2300 pulses. Due to interference, we ignore the last 223 pulses here.

Table 2. Mode Changes in B0943+10 and B1822–09 Observations

MJD	Modes	[a]Switch (pulse)	Length (in pulses)
AO B0943+10			
48914*	B to Q	816	986
52709*	Q to B	2540	6748
52711	B	–	6809
52832	Q to B	5266	7559
52840	B	–	7275
52916	Q to B	1755	6560
52917	B	–	3024
53491	B	–	5841
53492	B	–	6825
53862*	B	–	5041
54016	Q	–	6012
54630	B	–	7569
54632	Q to B	[b]3100	6656
GMRT B1822–09			
53780	B to Q	200	2077
	Q to B	770	
	B to Q	1095	
	Q to B	1200	
	B to Q	1475	
	Q to B	1755	
54864	Q	–	2106

* Sidebands surrounding the primary modulation feature are observable in the fluctuation spectra of these observations (See §III).
[a]Because the mode changes of B1822–09 occur over several pulses, these values represent an approximate boundary of the switch.
[b]This represents an approximation because of interference at the mode switch boundary.

the context of the 'rotating carousel' model, we must then ask what produces these observed sidebands. They are expected to occur if there is variation in the subbeam spacing or amplitude, which would result in their spacing around the primary modulation feature being harmonically related to the true drift-modulation frequency (f_3). While the observed f_3 (0.46 cycles per stellar rotation period, P_1) is not related to the sideband spacing (0.027 cycle P_1^{-1}), its first-order alias (0.54 cycle P_1^{-1}) is almost exactly 20 times the sideband spacing. This harmonic relation supports interpretating the observed primary modulation as a first-order alias of the true feature, and it indicates that the carousel is composed of 20 discrete 'beamlets.' (Paper I)

Independent evidence agrees with a carousel of 20 subbeams, in turn supporting the conclusion of aliasing. From the change in the polarization angle of the profile corresponding to the subpulse separation (P_2), and from viewing geometry considerations, Paper I determined that the beamlet spacing around the carousel is $\sim 18°$. $360°/18°$ then indicates 20 beamlets. Furthermore, Papers I & II both found a feature in the fluctuation spectra at ∼0.07 cycle P_1^{-1}, which is compatible with its being an alias of the second harmonic of the true primary fluctuation feature (0.54 cycle P_1^{-1}). Paper II also discovered a low frequency feature at 0.027 cycle P_1^{-1}, which corresponds to 1/20 f_3 if the observed primary feature is an alias. It was therefore concluded that the sidebands represent a modulation of the aliased primary modulation feature. However, an important consideration in understanding the physical origin of the observed fluctuation spectra was left unresolved: how often and under what circumstances do the sidebands appear?

From P_3 (the inverse of f_3), the total circulation time of the subbeam carousel is thus easily calculated as 20 P_3, or ∼37 times the stellar-rotation period (P_1). According to the polar cap emission theory of Ruderman & Sutherland (1975), the observed subbeam carousel is thought to result from "spark"-induced columns of relativistic primary plasma directed into the 'open' polar flux tube and precessing around the magnetic axis under the action of $\mathbf{E}\times\mathbf{B}$ drift.

Paper III (Rankin, Suleymanova & Deshpande 2003) extended the findings and methods of the first two papers using a number of simultaneous 103/40-MHz observations acquired on 16 different days at the Pushchino Radio Astronomy Observatory (PRAO).

Paper IV (Rankin & Suleymanova 2006) introduced several of the long (2+ hours) 327-MHz observations discussed in this paper, which allowed the discovery of orderly, correlated changes in the pulsar's average profile shape and the subpulse drift rate (and correspondingly, the circulation time).

Paper V (Suleymanova & Rankin 2009) reported on a new series of simultaneous PRAO 112/62 and 112/42-MHz observations. Changes in polarization were detected, with the linear polarization increasing from 10% at 'B' mode onset to 40-50% by 'B' mode cessation, over the course of several hours.

In this paper we continue our analysis of B0943+10 and compare its behavior to that of another famous mode-switching pulsar B1822–09. Several basic similarities between the stars allow further analysis to proceed: both have comparable periods (1.098 s for B0943+10; 0.769 s for B1822–09); and both have estimated surface magnetic fields on the order of 10^{12} G (ATNF Pulsar Database). Both are detectable as X-ray emitters, which is intriguing for two stars, each roughly a kiloparsec away and rotating with a

Table 3. Modal characteristics of B1822–09 and B0943+10

	B0943+10		**B1822–09**	
Mode	B	Q	Q	B
Luminosity	x mJy	y mJy	xx mJy	yy mJy
Interpulse?	—	—	✓	×
Precursor?	×	✓	×	✓
Regular modulation?	✓	×	✓	×
A(2/1) secular decrease?	✓	×	✓	×

∼1-sec period (Zhang, Sanwal & Pavlov, 2005; Alpar, Guseinov, Kiziloglu, & Öegelman 1995).

More important are the remarkable modal similarities between these two pulsars. B1822–09 has fascinated researchers because of its several discrete behaviors. Like B0943+10, it switches between two modes (Fowler *et al* 1981; Gil *et al* 1994): its so called 'Q'uiescent mode, which exhibits regularly drifting subpulses (as in the 'B' mode of B0943+10) and an interpulse; and its 'B'urst mode in which a bright precursor component turns on, the regular modulation disappears (as in the 'Q' mode of B0943+10)[1], and the interpulse turns off.

Nonetheless, the anti-correlation between B1822–09's interpulse and precursor (hereafter IP and PC; Fowler & Wright 1982) presents a difficulty for current emission models: if B1822–09 is a nearly orthogonal rotator, as has been argued, how does information transfer from one magnetic pole to the other? It has even been argued that the IP and PC originate from the same emission region which reverses emission direction in its two modes (Dyks, Zhang & Gil 2005).

In §II we describe the observations of B0943+10 and B1822–09 used in this paper.

In §III we outline the results of a new analysis of over 14 hours of 'B' mode observations from which we conclude that the important 'sideband' features discovered in Papers I & II occur relatively rarely.

In §IV we report the discovery of a 'precursor' component in B0943+10 (hereafter PC). Motivated by the presence of an IP in B1822–09 we have conducted a search for such a feature in B0943+10. This search has proven unsuccessful, but given the weakness of B1822–09's IP, a similar interpulse would appear absent for even a slightly different sight-line traverse, and given the weakness of B0943+10, a dim interpulse could be washed out in the noise.

In §V we report a study of two GMRT 325-MHz observations of B1822–09, the first ever in-depth analysis at meter wavelengths. Fluctuation-spectral evidence is reported suggesting that the main pulse (hereafter MP) and IP are linked, contrary to the Dyks *et al* reversal model. We find that B1822–09's modal behaviors, profile forms, and the polarization properties of its MP and PC are comparable to those of B0943+10. And like B0943+10, B1822–09 never seems to null. We further argue that B1822–09 is indeed an orthogonal rotator.

In §VI we discuss the implications of these findings, and review the case available for assimilating the properties of B1822–09 and B0943+10. In particular, the PC emission in both stars appears to be of neither the conal or core type, and its geometry could associate it with the so-called "outer gap" where the high-energy emission from pulsars is thought to originate.

II. OBSERVATIONS

The B0943+10 observations used in our analyses were made using the 305-m Arecibo Telescope in Puerto Rico (hereafter AO). The 327-MHz (P band) polarized PSs were acquired using the upgraded instrument together with the Wideband Arecibo Pulsar Processor (WAPP[2]) on a number of different days over a four-year period as detailed in Table 1. The auto- and cross-correlations of the channel voltages were three-level sampled and produced by receivers connected to linearly (circularly during the MJD interval 53289 to 54629) polarized feeds. Upon Fourier transforming, sufficient channels were synthesized across a 25-MHz (50-MHz after 54630) bandpass, providing resolutions of approximately 1 milliperiod of longitude. The Stokes parameters have been corrected for dispersion, interstellar Faraday rotation, and various instrumental polarization effects. Some of the PSs have been discussed in previous papers in this series; however this paper presents the 7 days of 2+ hour observations since MJD 53491.

The two observations of B1822–09 were carried out using the Giant Meterwave Radio Telescope (hereafter GMRT) near Pune, India, using the same techniques as described in Mitra, Rankin & Gupta (2007).

The spectral analysis techniques utilized in this paper were first presented and explained in detail in Paper I. We would ask the reader to refer to that paper for a complete description.

III. SIDEBANDS IN B0943+10

An important finding of the first paper in this series was the presence of sidebands surrounding the primary subpulse drift-modulation feature. Both the sidebands and the primary feature arise only during the 'B' mode. As argued in Paper I, these sidebands, shown in the longitude-resolved fluctuation (hereafter LRF) spectra of Figure 1, represent a "tertiary" modulation of the phase-modulated "drift" feature. Unless all the subbeams are perfectly identical in their amplitude and spacing—or are totally random—we would expect to detect such a tertiary periodicity corresponding to the rotation period (or circulation time) of the entire carousel, $\hat{P}_3$. Using the 430-MHz observation, Paper I determined these sidebands to fall symmetrically at 0.02680 $\pm$ 0.00037 cycle P_1^{-1} above and below the primary feature

[1] In this paper we choose to continue the terminology established by Fowler *et al* for the stars' two modes. The 'B' mode of B0943+10 exhibits behaviors such as drifting subpulses similar to the 'Q' mode of B1822–09, while the 'Q' mode of B0943+10 and the 'B' mode of B1822–09 both display a precursor (see Table 3) The names derive from the relative intensity of the two modes and do not represent the most physically significant properties. In short, the 'B' mode in one star does not correspond to the 'B' mode of the other.

[2] http://www.naic.edu/~wapp

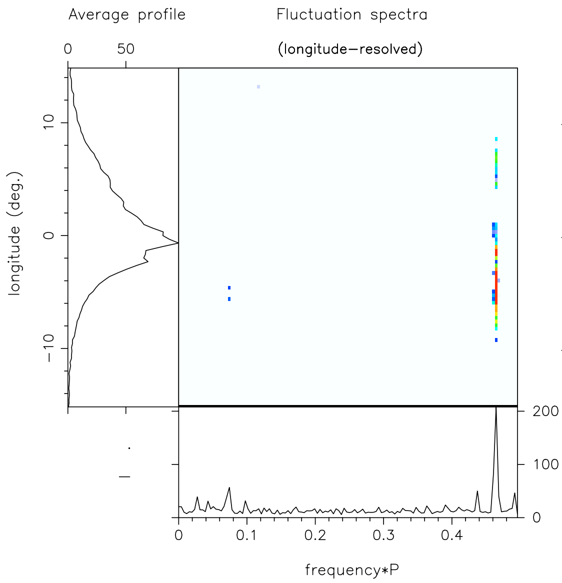

Figure 1. ‘B’ mode Longitude-resolved fluctuation (hereafter LRF) spectra for the MP of B0943+10 at 430 MHz, averaged over pulses 106-361 of MJD 48914 using a 256-point FFT. The average profile is given at the left of the figure and the integral spectrum is at the bottom. The central panel shows the amplitude of the features. This is the first known instance of sidebands surrounding the primary modulation feature of B0943+10. It was studied at length in Paper I. At about 0.026 cycle/P_1, the sideband spacing represents an harmonic relationship with the first-order alias of the large primary modulation feature, providing evidence that the pattern of drifting subpulses in B0943+10 comes from a rotating carousel of 20 “sparks” of bright emission. The intensity scale is arbitrary.

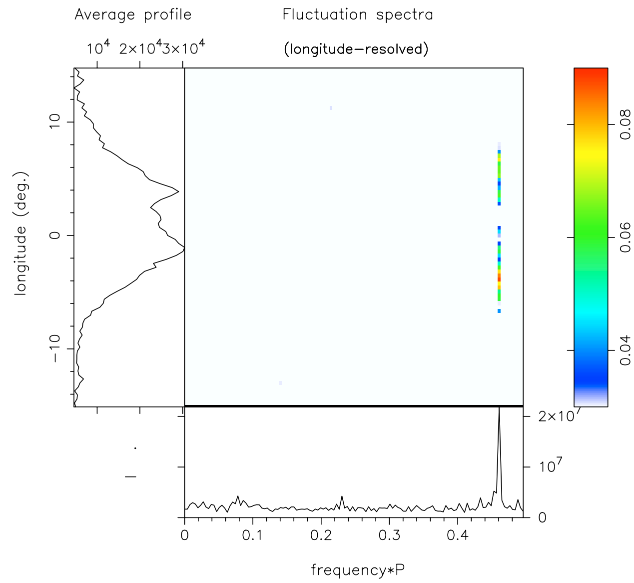

Figure 2. ‘B’ mode LRF spectra (as in Fig. 1) for the MP of B0943+10 at 327 MHz, averaged over pulses 4085-4340 of the MJD 52709 PS using a 256-point FFT. Weak sidebands are present, surrounding the main feature; their remarkably even spacing and their persistence over several hundred pulses allows us to conclude that they represent a physically significant modulation of the primary feature at some 0.46 cycle P_1^{-1}. Note also that the primary feature strongly modulates the two subcomponents, while the center of the profile is much less modulated.

at 0.535 cycle P_1^{-1}. That they are so symmetric and narrow indicates a regular amplitude modulation (of the phase modulation).

The brevity of the 430-MHz observation analyzed in Paper I left unresolved an important consideration: how often do these sidebands arise? We are now able to report the results of an analysis based on a wealth of observations, and we find that these sidebands are rarely present in B0943+10. They are in fact only known to occur on three separate occasions: on MJD 48914 in Paper I at 430-MHz (see Fig. 1); and in the 327-MHz observations on MJD 52709 and MJD 53862 (see Figures 2 & 3). Out of some 58,000 ‘B’ mode pulses now available in the AO PSs—comprising more than 18 hours of observations—sidebands can be discerned in fewer than 3,000. When they do appear, the sidebands are stable for several hundreds of pulses—which indicates that this tertiary modulation can persist over many times the 37-P_1 carousel circulation time—and yet they vanish for many hours at a time, and they never seem to persist for more than about 18 mins.

We can conclusively corroborate several of the findings of Paper I. The sidebands never appear to be accompanied by any other pairs, nor is there evidence of any other tertiary modulation of the primary feature in pulse sequences where the sidebands are not present. The pair of modulation features are always remarkably evenly spaced, the difference in their spacings from the primary feature always being less

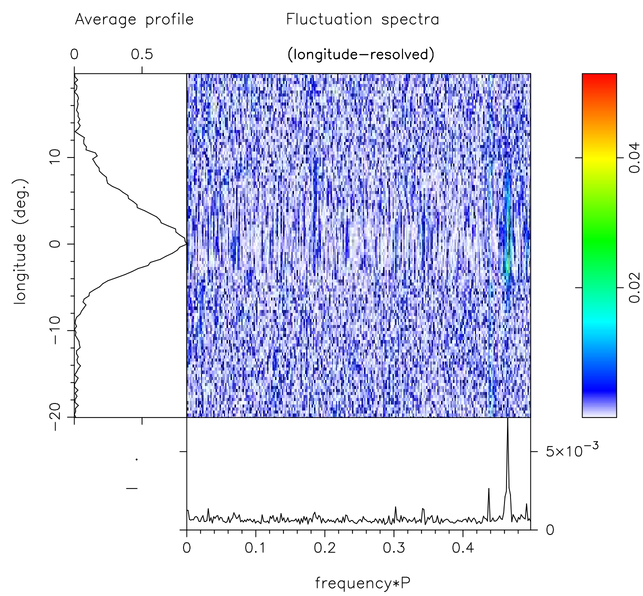

Figure 3. ‘B’ mode LRF spectra (as in Fig. 1) for for B0943+10 at 327 MHz, averaged over pulses 260-771 of the MJD 53862 PS using a 512-point FFT. The stability of the sidebands in this observation allowed us to measure their spacing with high precision. We were able to average over 512 pulses without washing out the modulation, allowing use a 512-point FFT. Whereas before the sidebands were symmetric, in this observation one is clearly ‘taller’ than the other.

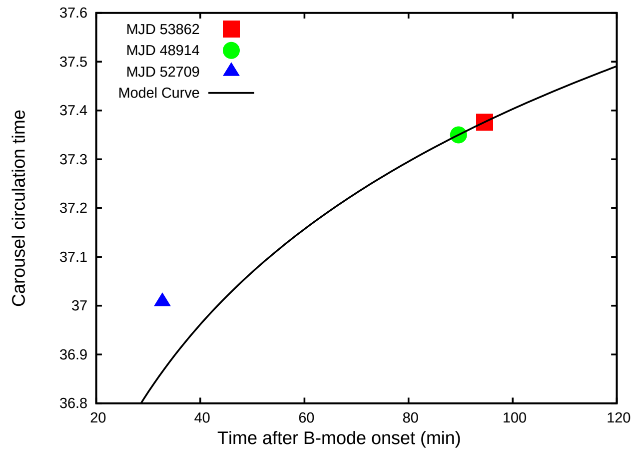

Figure 4. $\hat{P}_3$ *vs.* the time after 'B' mode onset of the three known occurences of sidebands in B0943+10 are plotted above, along with a model curve representing the relationship established in Paper IV: $t = 1.826 \times 10^{-32} \exp[2.077\hat{P}_3]$. There is no discernible relation between the sideband occurrence and the evolution of the 'B' mode. The time positions of the MJD-48914 and 53862 observations are calculated from $\hat{P}_3$, and should be considered estimations; signficant deviation from the model curve is expected, but not plotted here.

than 3% of their actual spacing. The inverse of this spacing remains commensurate with the carousel circulation time calculated as 20 P_3, though the agreement is stronger in the 430-MHz observation than in the others.

In the MJD 52709 observation (see Fig. 2), the sidebands occur during a roughly 550-pulse interval, during which $\hat{P}_3$ determined from the alias of the primary modulation feature is 37.008±0.013 P_1. In agreement with the findings of Paper I, these sidebands are of nearly identical height, implying an amplitude modulation. In the MJD 53862 observation, sidebands are detectable for some 1000 pulses (see Fig. 3). $\hat{P}_3$, measured from the primary modulation feature, is 37.376±0.005. One interesting difference is present in this observation: the sidebands are significantly asymmetric; the 'right' sideband is only 63% the height of the 'left' one. This indicates a mixture of amplitude and phase modulation.

Aside from the rarity of the sidebands, a significant finding is that their appearance seems in no way correlated with the evolution of the 'B' mode. In the 430-MHz observation, the sidebands appear at the end of a 'B' mode episode, immediately before the transition to the 'Q' mode. In the MJD 52709 observation, sidebands appear only about 28 minutes after 'B' mode onset. Then, sidebands appear for 18 minutes at the beginning of the MJD 53862 observation, and disappear for its remaining 74 minutes (all in 'B' mode). Using two relationships established in Paper IV, we can estimate how long after 'B' mode onset the beginning of this observation lies. (a) $t = -\tau \ln[(A(2/1) - 0.17)/1.16] = \sim 100$ min, where A(2/1) is the amplitude ratio of the two components comprising the MP, and τ is the characteristic time of some 73 min. (b) $t = 1.826 \times 10^{-32} \exp[2.077\hat{P}_3] = \sim 95$ min. These computations are only approximate, but we can conclude that in the MJD 53862 observation, the sidebands

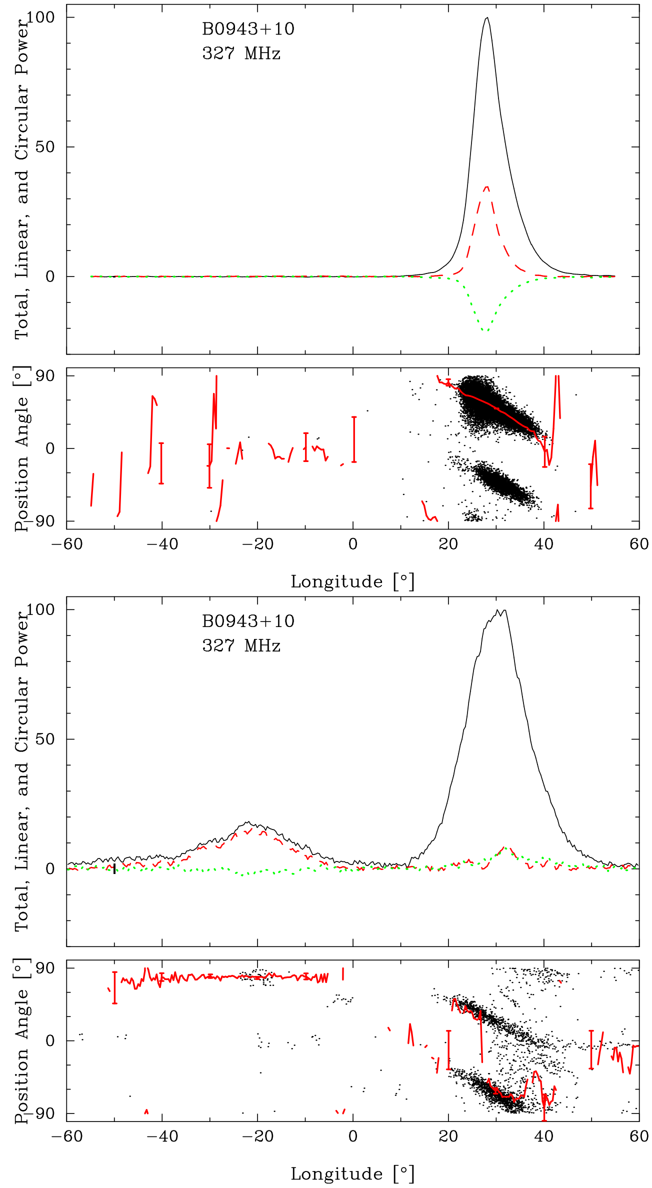

Figure 5. Polarization profiles and PPA histograms for B0943+10's 'B' (4000 pulses from MJD 53492) and 'Q' (1050 pulses of MJD 52832) modes, respectively. **'B' mode (top)**: here the MP retains significant PPM power, and its PPA traverse is well defined. The PPA regularity around –25°, which is only seen in very long integrations, apparently represents weak SPM PC power in its 'off' state. **'Q' mode (bottom)**: The MP is almost completely depolarized by nearly equal levels of OPM power (visible as parallel "tracks" in the PPA distribution, separated by 90°). The PC, however, is highly linearly polarized, with almost no circular polarization. Note the unusual flat PPA traverse. The upper and lower panels display the total power (Stokes I), total linear polarization (L [$=\sqrt{Q^2+U^2}$]; dashed red) and circular polarization (V [LH-RH]; dotted green) (upper), and the polarization angle (PPA [$=\tan^{-1}(U/Q)$]) (lower). Individual samples that exceed an appropriate >2 sigma threshold appear as dots with the average PPA (red curve) overplotted. The PPAs are approximately absolute (see text). The intensity scale is arbitrary.

show up around an hour further into 'B' mode than they do on MJD 52709 (see Fig. 4).

IV. PRECURSOR DISCOVERY IN B0943+10

We now introduce the newly discovered presence of a 'precursor' component in B0943+10 which occurs strongly only in the 'Q' mode. Measuring from the center of the half-power point, the PC lies 52° before the MP, as can be seen in the lower panel of Figure 5. Because previous analyses of B0943+10 have focused almost exclusively on its 'B'-mode characteristics, most "working" PSs were restricted for convenience to a 40-60° window surrounding the MP; and when not the occasionally present emission in the 40°-longitude range of the PC was at first dismissed as interference.

During the 'B' mode, the PC emission levels are comparable to the noise level, resulting in an integrated profile in which the precursor appears absent (see the top plot of Fig. 5). During a 'Q'-mode interval, the PC is ∼18% of the intensity of the MP (which is itself both weaker and broader than in the 'B' mode). Though weaker, the PC is actually some 1.67 times wider than the MP at half power (∼25° and ∼15°, respectively). Weak emission from each component is detectable for ∼45°. The PC switches off immediately at 'B' mode onset, producing no emission above the noise level. We have no full-longitude observations of the 'B'-to-'Q' mode transition, so the behavior of the PC at this boundary is unknown.

While the PC and the MP are regulated by the same modes, their properties and behaviors are otherwise distinct. During the 'Q' mode, when the PC is most prominent, its emission is nevertheless sporadic. Individual pulses are composed of many short spikes of emission, as shown in Figure 6, and are typically difficult to distinguish from the noise. It is possible that the PC and the 'Q'-mode MP null, but the sporadic pulse shapes and low intensity of the PC make analysis of individual pulses difficult in our observations: nulls simply cannot be distinguished from noise fluctuations. As was pointed out prominently in Paper I, the MP is itself more sporadic in the 'Q' mode than in the 'B' mode, but it is still comprised of recognizable subpulses as opposed to the PC. Individual pulses vary greatly, but MPs are composed of a few, comparatively 'smooth' subpulses which are much broader than those seen in the PC. Conversely, the elements of PC emission have durations about equal to the sampling time and appear similar in character to the PC emission in B1822–09 (see Gil *et al* 1994: fig. 5) and the emission of B0656+14 (Weltevrede *et al* 2006b: see fig. 4). Clearly, the PC is weak on an individual-pulse basis and affected by noise fluctuations, but the noise cannot account for its different character.

During the 'Q' mode, integrated profiles of the MP have almost no linear or circular polarization. As demonstrated in SIRR, this results from nearly equal power contributions by two orthogonal polarization modes (hereafter OPMs). Individual pulses contain significant linear polarization, but when aggregated, the polarization disappears. Accounting for the 90° separation of the two OPMs, the MP has a prominent linear PPA traverse of –1.7°/° longitude.

The PC is highly linearly polarized (85% at the peak); there is clearly one dominant OPM. Most perplexing is that within the errors, the PPA traverse is flat: 0 °/° longitude. This strongly suggests that, unlike the MP, the PC is not a conal component.

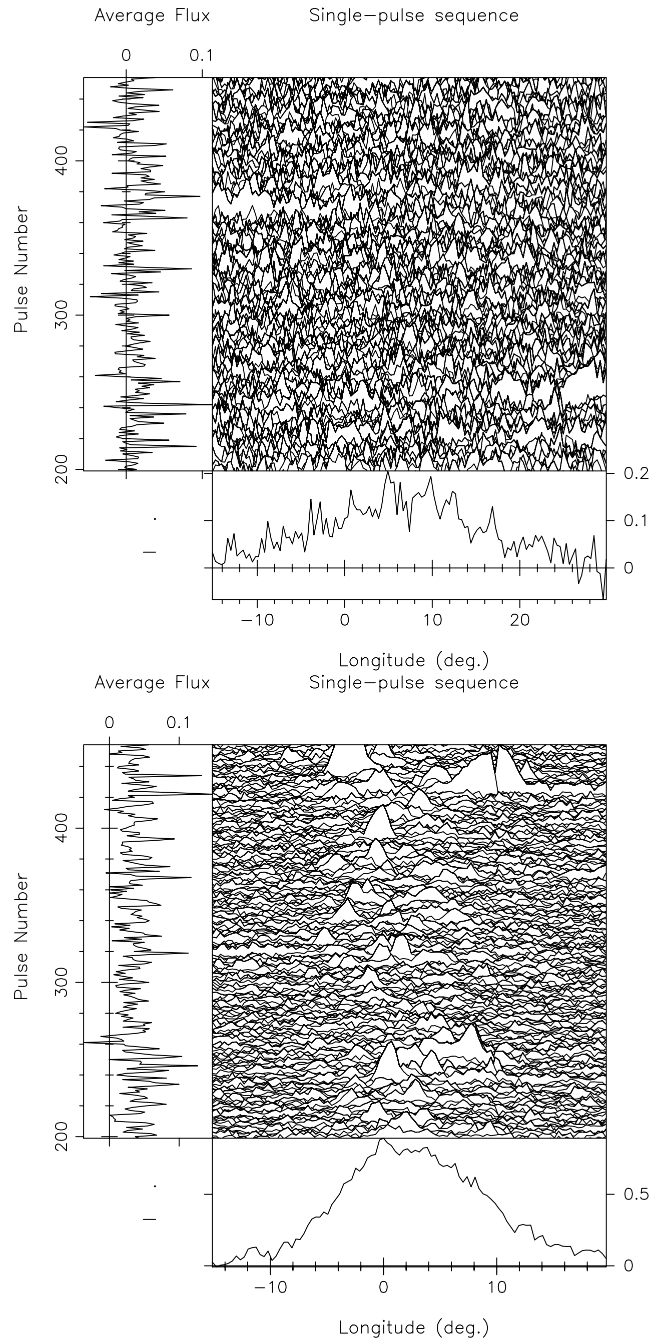

Figure 6. A 256-pulse sequence, taken from the MJD 52832 observation. The precursor (top) and main pulse (bottom) in the 'Q' mode of B0943+10. The individual PC pulses are composed of many small spikes of emission, while the individual pulses of the MP are comprised of fewer, broader subpulses. The intensity scale is arbitrary.

At 'B' mode onset, both components undergo drastic changes. The main pulse exhibits its well known modulation features discussed throughout this series. Drifting subpulses appear so rapidly that we are able to determine the time of the modal switch down to a single pulse (or two). One

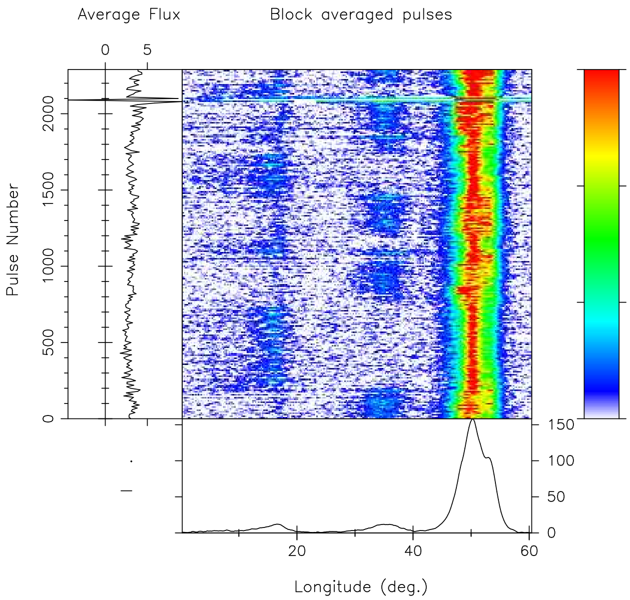

Figure 7. The full 2300-pulse B1822–09 observation on MJD 53780 in 10-pulse averages. The PC and MP components (on the right) are located at their actual relative longitudes; whereas the IP (on the left) is spliced into the plot prior to relative longitude +23° for convenience (exactly 140° of longitude is removed at this point.) Some 30 pulses around 2100 are corrupted by RFI, thus our further analyses will use only 2077 pulses. The intensity scale at red saturates the MP (and is biased positively) in order to better show the IP and PC mode-changes. The anti-correlation between the IP and the PC is very clearly shown. When one is 'on,' the other is 'off.' Note that the MP structure broadens in the 'B' mode when the PC is present; whereas in the 'Q' mode the 43-P_1 modulation is readily discernible in the IP.

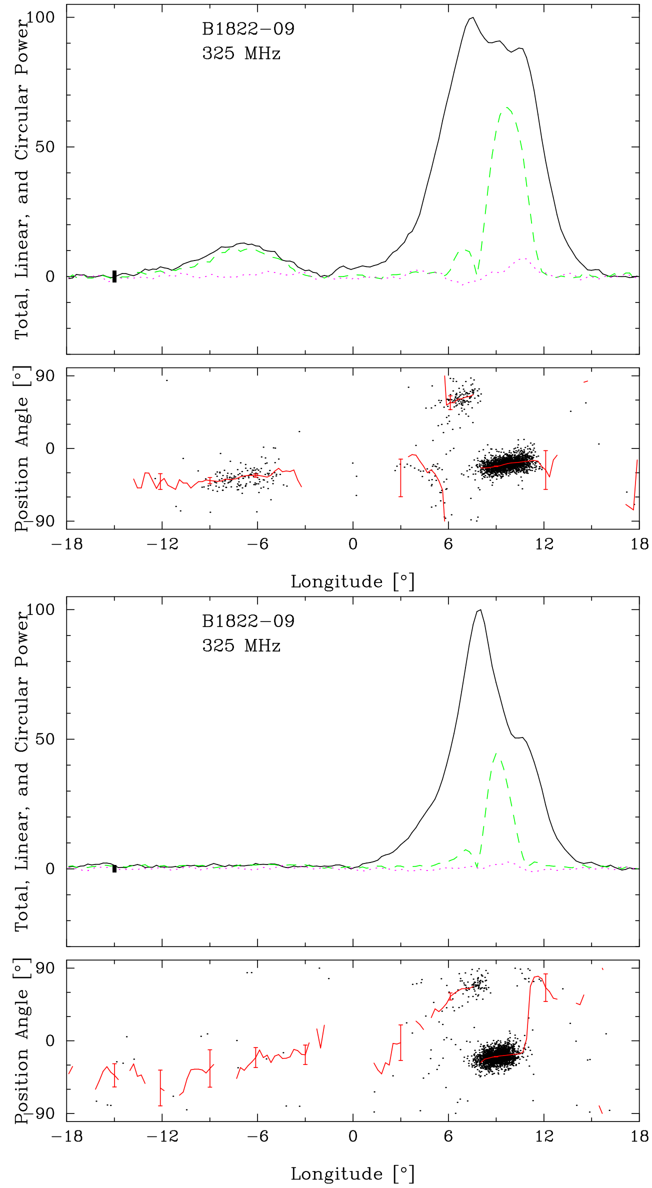

Figure 8. Average profiles and polarization histograms of the PC and MP of B1822–09 during its 'B' (pulse #s 1200-1455) and 'Q' (#s 200-770) modes, in Fig. 7, respectively. **'B' mode (top)**: here the highly linearly polarized PC 'turns on,' and its nearly flat PPA traverse is remarkable. Accounting for the 90° OPM "jump", the MP PPA is also essentially flat, suggesting a nearly central sightline traverse. **'Q' mode (bottom)**: the conal components flanking the central MP feature have reduced intensity, so the profiles is narrower. PC emission is still faintly visible, along with a trace of its linear polarization. The quantities plotted are the same as in Fig. 5.

of the OPM dominates, resulting in an average profile with significant linear polarization: about 10% at 'B' mode onset, increasing to 40-50% by 'B' mode cessation (see Paper V). The PC, by contrast, shuts off almost completely during the 'B' mode. Because of the weakness of the PC, it is impossible to determine how quickly its emission drops off with anything like the same precision as the modal changes in the MP.

Despite its weakness during the 'B' mode, a trace of the PC can still be detected through its linear polarization. In integrations of several thousand pulses, we see nothing of the PC in total power, but enough L remains to define its PPA (see Fig. 5). Over some 20° of longitude where the PC was present during 'Q' mode, we now see highly polarized 'noise,' with the flat traverse characteristic of the PC. Note the contrast with the other PPAs outside of the PC and the MP that are random, as is expected of actual noise. Interestingly, this residual 'B' mode PC polarization is orthogonal to that of its 'Q' mode counterpart, arguing that it is the SPM being seen here.

V. METERWAVE STUDY OF PULSAR B1822–09

As we have outlined above, pulsar B1822–09's mode-associated PC component and IP have attracted great interest and have prompted extensive and repeated study over the years. Virtually all previous single-pulse analyses of B1822–09 have been carried out at frequencies above 1 GHz and usually with the Effelsberg telescope (*e.g.*, Fowler & Wright 1982). Nonetheless, its tripartite profile and PPA traverse has proven difficult to interpret geometrically, and no existing study has provided a fully satisfactory model.

Our interest in B1822–09 was prompted by its ostensible similarity to B0943+10. In order to explore this similarity fully, however, we find we need both to conduct some new analyses of the star's PSs and to interpret them in the context of an understanding of its emission geometry. In particular, we have carried out the first in-depth analysis of B1822–09 at meter wavelengths, but even here we can make no easy assumptions about fully exploring the pulsar's effects because our two GMRT 325-MHz observations exhibit drastically different modal behavior. The MJD 53780 PS displays the star's characteristic mode-switching behavior: the two modes each endure for several minutes (around 200-500 pulses), with the overall profile being comprised fairly equally of both modes (see Figure 7). The MJD 54864 total-power PS, however, displays an hitherto unknown B1822–09 behavior: a 2106-length PS is composed entirely of the 'Q' mode, never once switching to the 'B' mode. Though much longer than usual, this 'Q'-mode PS otherwise appears perfectly normal.

Figure 7 shows the full 2300-pulse observation of MJD 53780 in 10-period averages; note that exactly 140° of longitude have been removed at +23°, so that all three emission features, the IP, PC and MP appear in this sequence. The multiple modal transitions are obvious. B1822–09's 'Q' mode is characterized by the presence of its IP, along with a strong low frequency modulation feature. During the 'B' mode, the IP and the regular modulation cease almost completely, and a PC some 15° before the main pulse 'turns on'. The figure also shows greater breadth and complexity in the MP during the 'B' mode, that partially accounts for its greater aggregate intensity. Finally, note that about 30 pulses are corrupted by interference near the end of the PS, thus we will restrict all of our analyses to the first 2077 pulses.

Partial profiles corresponding to the two modes are given in Figure 8. The nearly complete linear polarization of the PC feature in the 'B' mode (upper) is well known, but striking in contrast to that of the MP. Note also that the PPA traverse of the PC is very flat, and that correlated PPAs at similar angles in the 'Q'-mode profile (bottom) show that some PC power remains. In fact, there is no strong evidence of PPA rotation throughout the profile: here we see only PPAs that are around –40 and +50° that presumably represent the two OPMs, and the same conclusion follows even for the largely depolarized IP [not shown, but see Gould & Lyne (1998) at 1642 MHz]. Finally, the forms of the 'B'- and 'Q'-mode partial profiles are dramatically different: Many total MP profiles show little structure, and care is needed in separating the modes to reveal the different contributions to MP power [*e.g.*, see Gil *et al* (1994): fig. 1]. Indeed, on the basis of the modal profiles here, we can only be sure that the MP *has* parts—that is, a bright central component as well as both a leading and trailing emission region. Stronger evidence to this effect we already saw in Fig. 7, where fairly steady central-component power occurs together with leading and/or trailing emission.

Finally, Figure 9 shows a longitude-longitude correlation map for the entire 2077-pulse length of the MJD-53780 PS at a 2-P_1 delay. As we saw in Fig. 7 this observation is comprised of about equal contributions of 'B' and 'Q'-mode intervals, so the map mixes the behaviours of the two modes. Note, however, the strong correlations between the two sides of the MP and the other emission zones. This is seen over all delays of a few pulses, and the nearly identical maps for negative and positive delays on either side of the diagonal are compatible with amplitude modulation. The

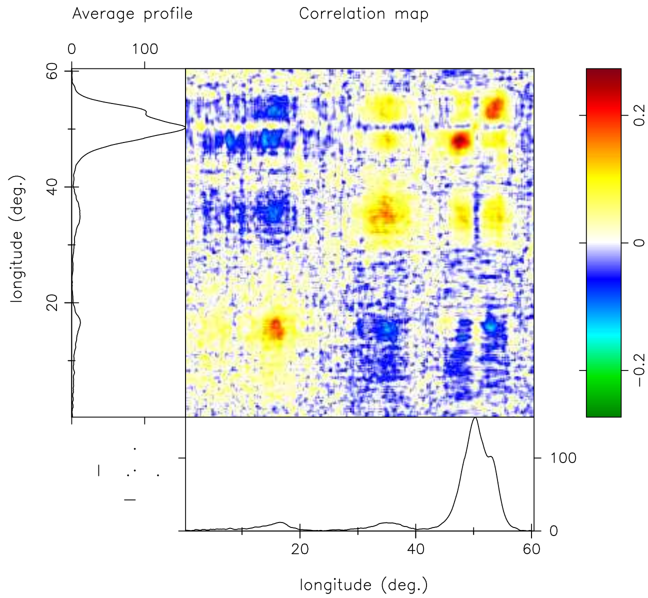

Figure 9. Cross-correlation map of the MJD-53780 PS with itself at a delay of $2P_1$ calculated over the entire 2077 pulses, including both modes. The main panel shows the correlation between different longitudes as marked by the profiles in both the side and bottom panels. The leading and trailing edges of the MP are positively correlated with each other and the PC (and negatively correlated with the IP), whereas the center of MP correlates with neither. This strongly indicates that the MP has a three-zone emission structure, although this is not fully clear from its average profile. The ordinate is delayed with respect to the abscissa, and the positive (negative) delay maps are shown below (above) the diagonal; these two maps are virtually identical, indicating correlations that are time-reversable. The three-sigma error in the correlations is about 6%.

PC correlations with the sides of the MP reflect the greater MP activity in these regions during the 'B' mode when the PC is present; the negative correlation with the IP, shows the opposite in the 'Q' mode.

1. 'B'urst mode in B1822–09

Our observations provide only the four brief 'B'-mode apparitions seen in the MJD-53780 observation of Fig. 7. Fluctuation spectra of these intervals show no significant periodicities. A weak 'B'-mode modulation feature corresponding to about 11 P_1 has been reported at higher frequencies (*e.g.*, Gil *et al* 2004), but we find no evidence at all of such a modulation in our 325-MHz fluctuation spectra in any of the components. Also, a cross-correlation map similar to Fig. 9 (not shown) for the 'B'-mode interval of pulses 1200-1475 shows no significant correlation between the PC and MP emission regions.

The 'B' moniker in the literature derives from its greater MP intensity. Much of this enhanced power owes to its broader profile, which in turn is due to its stronger leading and trailing components. At 'B'-mode onset, the pulsar's IP switches off almost completely, while a PC switches on. The intensity of the PC is much less frequency dependent than that of either the IP or MP. At high frequencies above 1

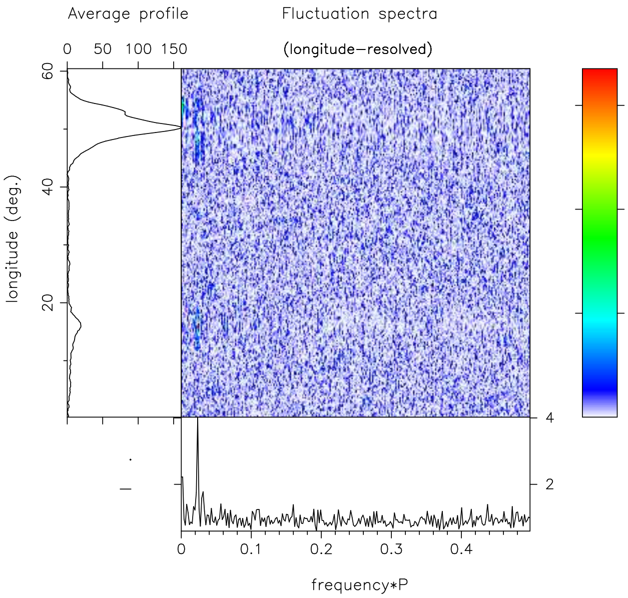

Figure 10. Longitude-resolved fluctuation spectra of pulsar B1822–09's 'Q' mode, averaged over pulses 221-750 of the MJD 53780 observation, using a 512-point FFT. The MP is at the top of the left-hand panel, the PC in the center, and the IP at the bottom. A strong feature at 0.023 c/P_1, corresponding to a P_3 of about 43 P_1, modulates both the MP and the IP, while the weak PC displays no discernible modulation.

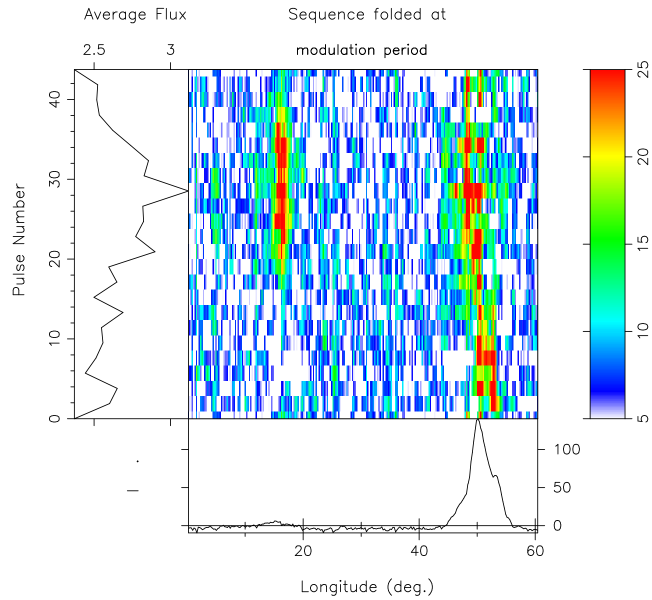

Figure 11. 'Q'-mode PS from Fig. 7 folded at the primary modulation period. Pulses 221-750 of the MJD 53780 observation are folded at 43.75 P_1 corresponding to the bright modulation feature in Fig. 10. Here the unvarying 'base' has been removed from the power in the central panel and the colour-scale compressed both at small and large intensities. The modulation affects both the IP and MP (see the average profile in the bottom panel), producing primarily an amplitude (stationary) modulation in the IP and a phase modulation in the MP: note the way in which the fluctuation power appears at only one phase in the IP; whereas, in the MP fluctuation power appears in both the leading and trailing regions of the profiles at different phases.

GHz, the MP becomes progressively dimmer compared to the PC (Gil *et al* 1994). Averaged over the four 'B'-mode intervals, we find the PC 's peak intensity to be 12% that of the MP.

The linear polarization of the PC is nearly complete and thus remarkably different from that of the MP (see Figure 8). This large L/I extends across its entire width, such that nearly all of its power is in a single OPM. Its PPA traverse is linear and nearly flat with a slope somewhere between 0 and $1.3^\circ/^\circ$.

The MP form and polarization structure is more typical. Its edges are completely depolarized, apparently by the usual OPM activity; whereas the middle of the MP shows a broad region of significant fractional linear that is divided by a 90° OPM-dominace "jump". Overall, then, there is virtually no evidence for rotation of the PPA under the MP: the PPA under the leading part of the profile is essentially that of the well defined middle, and the "jump" at about $+7^\circ$ longitude is clearly OPM related. With respect to V, there is a weak anti-symmetric signature that is centered at about $+9^\circ$ longitude, but it is not clear whether this is significant.

We can now see clearly how it has been that B1822–09's profile is difficult to classify and interpret. Little can be made of its ostensibly "double" average MP profile, and the modal partial profiles in Fig. 8 are in turn quite complex. We find unassailable evidence for a basic tripartite form—leading, middle and trailing—but even the modal profiles show us no simple triplicity. That in the top panel of the above figure shows weak early and bright trailing emission around the central component, but other 'B' episodes in Fig. 7 have a reversed or more balanced character. If then the central feature is of the core type, which seems a sensible premise on multiple grounds, then the MP's 'B'-mode behaviour is suggestive of the T or M profile class and a highly central sightline traverse.

In this context, B1822–09's PC component is aberrant, in the sense that it has no clear interpretation within a current understandings of the possibilities of polar cap emission. Its flat PPA traverse and virtually complete linear polarization adds to this strangeness as does the character of its individual pulses. Gil *et al*'s (1994) fig. 5 plots a set of PC and MP single pulses with 50-μs sampling, and the difference between the respective two regions is startling: one sees no subpulses in the PC as its emission elements typically have widths of only a single sample. The MP emission, by contrast shows emission structures that are several degrees wide—the subpulses with which we are familiar. This "spiky" emission was also seen by Weltevrede *et al* (2006b) in B0656+14, where Patrick sometimes referred to its strikingly different character as "rain". Also, we have seen just above (see Fig. 6) that the B0943+10 PC has the same characteristic.

2. 'Q'uiescent mode

As we saw earlier in Fig. 7, the B1822–09 'Q' mode exhibits a strong and regular modulation affecting both its IP and MP. Its period there can readily be estimated at about 40 P_1 (see also Weltevrede *et al* 2006a). Figure 10 gives LRF

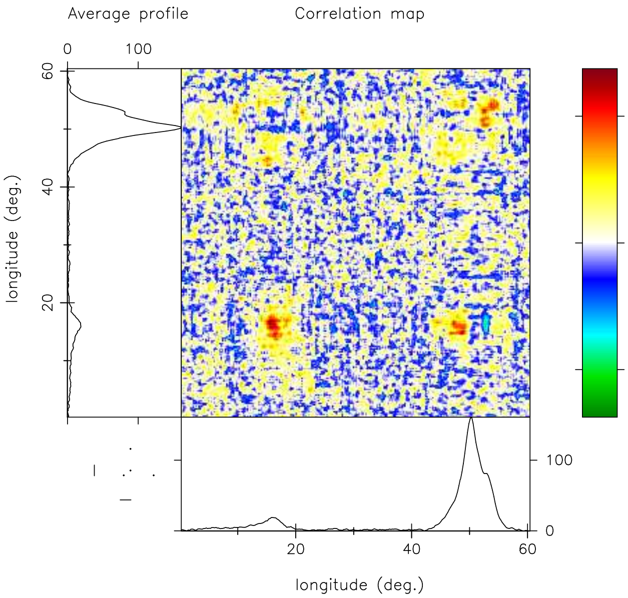

Figure 12. Cross-correlations of the PS with itself at a delay of $2P_1$, calculated over pulses 221-750 of the 'Q' mode-only MJD 53780 observation. Here we see a strong correlation of the IP with itself as well as a significant correlation of the delayed IP with the leading region of the MP profile, but not the reverse. Note also that it is a trailing region of the IP that is modulated, but a long leading region precedes it. The 3-sigma error in the correlations is about 13%. See Fig. 9 for details.

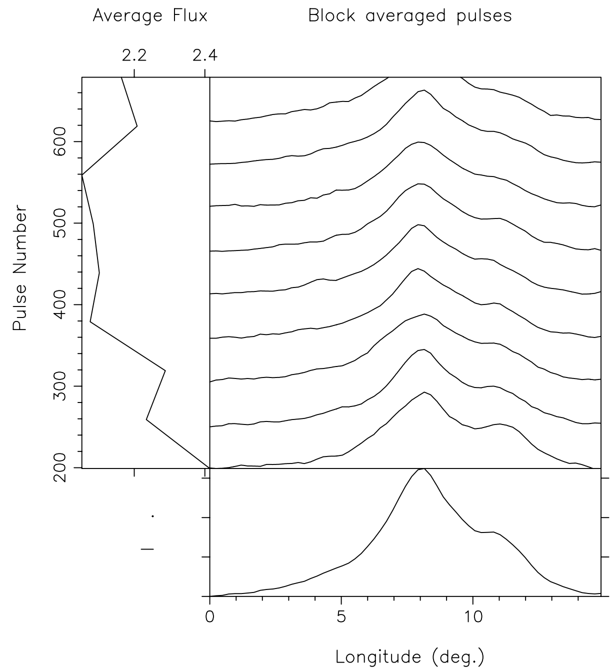

Figure 13. Profile-shape changes in the MP of B1822–09 after 'Q' mode onset, from the MJD 53780 observation. Each profile is an average of 60 pulses. Directly after the 'B'-to-'Q'-mode transition at about pulse 200, the profile has a prominent trailing component. At later times after 'Q'-mode onset, the leading profile region maintains a relatively stable intensity, while the trailing one gradually weakens.

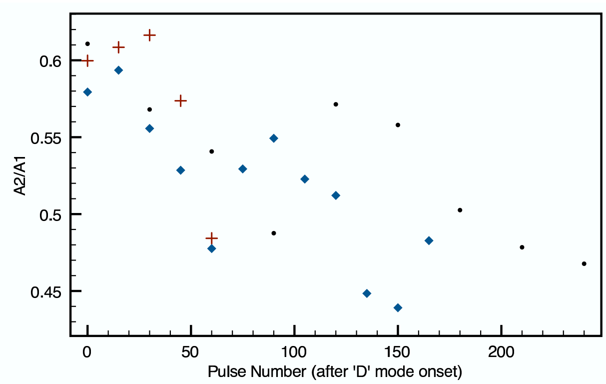

Figure 14. Changes in the trailing- ($A2$) to peak- ($A1$) amplitude ratio in the B1822–09 MP profile following 'Q'-mode onset. The amplitudes are measured from 30-pulse averages of the MJD 53780 observation. $A1$ is measured at the peak of the profile and $A2$ as the intensity $\sim 3°$ later, at the peak of the trailing component. First 'Q' mode apparition: black dots; second, red crosses; and third: blue diamonds.

spectra for the interval 221-750, and we see that the low frequency modulation produces a strong and narrow feature at 0.023 c/P_1. The feature modulates both the MP and IP strongly and corresponds to a P_3 of some 43 P_1. An harmonic-resolved fluctuation spectrum (not shown) shows that the feature represents a mixture of amplitude and phase modulation. Taking care to measure the primary period accurately by appropriately weighting two adjacent frequency components, we find a period of 43.75±1.0 P_1.

The effects of this modulation periodicity can be further explored by folding the 'Q'-mode PS at the 43.75-P_1 modulation period, and this display is shown in Figure 11. Here the unfluctuating 'base' power has been removed and the colour scale somewhat compressed to show the fluctuations more clearly. The IP is fully modulated at this periodicity, so we see its power in only a particular region of the full cycle. The MP, however, shows a "wobble" of fluctuation power extending from the leading to trailing regions of its overall profile. Power in the leading profile region occurs nearly simultaneously with power in the IP, whereas the trailing MP region is bright at times when the IP power is at a minimum.

Similarly, the longitude-longitude correlation map at a delay of 2 P_1 in Figure 12 shows significant correlation between the delayed IP and the leading regions of the MP; however, the map for the reverse (–2 P_1 delay) above the diagonal shows much less correlation. This asymmetry is characteristic of a phase modulation that has a "direction". Similar maps are obtained for other delays of a few periods. Note also that only a trailing region of the IP is modulated, but a long weak region of emission precedes it.

Finally, B1822–09's MP appears to exhibit secular changes over the several hundred pulses following 'Q'-mode onset. Figure 13 shows a set of 60-pulse averages following the first such onset in Fig. 7. Here we see that the power in the leading profile region remains fairly constant along with the intensity of the central component; whereas the power in the trailing profile region first exhibits a distinct component and thereafter declines progressively over the next 500 pulses. That the three long 'Q'-mode episodes in the MJD

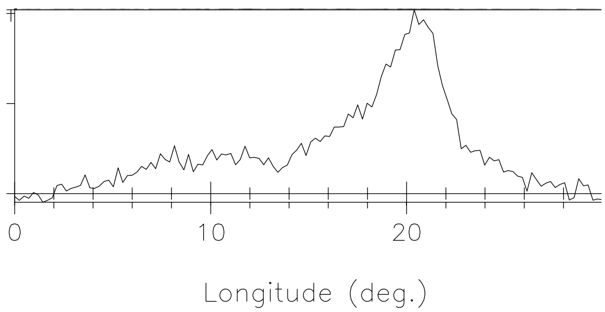

Figure 15. A close up average profile of the IP, averaged over all 2106 pulses of the MJD 54864 observation. Dyks *etal* measure the MP-to-IP separation as ∼186°, but if instead of measuring from the peak or the center of the half-power point, we measure from some 6° earlier—at the center of the IP—this separation reduces to almost precisely 180°.

53780 PS show a similar behavior is shown in Figure 14 where decreases of about 20% relative intensity are seen over 200 pulses in all three cases. Clearly, such a behaviour is very reminiscent of the changes seen in B0943+10 following its 'B'-mode onsets, but on a very much shorter time scale.

3. The emission geometry of B1822–09's PC & MP

As we have seen above, B1822–09 presents a "main pulse" profile that has been very difficult to interpret. First, it has not been clear whether the PC component was or was not a part of this "main pulse" region. Indeed, it has been tempting to regard it as so, because the PC and MP are connected by a weak bridge of emission that would ostensibly seem to associate them. Second, the MP structure itself is not at all clear in average profiles; some show hardly more than a single component with a trailing "bump", and at best one can discern two barely resolved components.

We now see clearly, however, that the PC is a completely different sort of "animal" than the MP: it is comprised of a very unusual and distinct kind of emission elements, and it is modulated very differently from the MP. It is truly and unmistakably a PC and not a part of the "main pulse". In short, it is almost certainly not of a conal origin.

Returning now to the MP, which indeed is the totality of the "main pulse", our various single pulse analyses have revealed that it is comprised of three very distinct regions, the leading, central and trailing regions. The central region has a half-power width of some 3° and shows a very steady emission from pulse to pulse. The leading and trailing regions, by contrast, are illuminated episodically and only occasionally at the same time—and in the 'Q' mode their illumination is periodic with the same 43-P_1 cycle as the IP. The illumination of these leading and trailing regions is responsible in large part for the greater intensity of the 'B' mode as is very clear from Fig. 7.

For all these reasons, then, there can be very little doubt but that the MP of B1822–09 should be classified as having a basically triple profile. In some partial profiles, we see a suggestion of two conal rings in the leading or trailing regions, which would suggest a five-component M profile, but such behaviour is not seen consistently enough to be certain. Moreover, the softer spectrum of the central component, its regularity, lack of periodic modulation (and correlation with other profile features), and the hint of antisymmetric V all suggest that this is a core component.

We can then apply the quantitative geometrical methods of ET VI to B1822–09's MP: Its PPA traverse shows no discernible rotation, so we can take its central slope to be essentially infinite—indicating that the sightline passes almost exactly over the pulsar's magnetic pole. The about 3° half-power width of the core further suggests a nearly orthogonal relationship between the star's rotation and magnetic axes as the angular width of the star's polar cap can be estimated as 2.8°. Thus the magnetic latitude α and sightline circle ι are both close to 90°.

With these constraints in mind, we can estimate what would be the total half-power angular sizes of the inner and outer conal regions and then compare them with the full width of the B1822–09 profile. These respective conal widths are about 9.5-10 and 13°. Referring conveniently to Fig. 14, we can see immediately that the full outside width of the leading and trailing regions cannot be squared with 13°, but a width of 9.5-10° corresponding to an inner cone is fully plausible. Therefore, we can conclude that B1822–09's MP is fully compatible with the inner-cone **T** classification.

4. The emission geometry of B1822–09's IP

Our analyses also shed new light on the IP and its relationship to the MP and PC. First, the IP is not a single symmetrical component, but rather a broad region of emission with a bright trailing component. Figure 15 gives a sensitive 325-MHz profile in which its somewhat double form and nearly 20° width are obvious. In the older publications of Fowler *et al* and Wright & Fowler, one gets little sense of its extended form, and even in the Gil *et al* work, the IP appears as a single asymmetric feature. Clearly, the early observations lacked our sensitivity, and perhaps the IP changes its form at meter wavelengths, but in either case its broad and asymmetric character must be taken fully into account.

The spacing of the IP from the MP is clearly shown in several of the previous figures, but the bottom panel of Fig. 7 depicts their spacings with respect to the PC as well. In this and the other diagrams, exactly 140° of longitude has been removed at longitude +23°, so the relationships between the three emission features can be measured conveniently. Most obviously, we see that the interval between the IP and MP peaks is about 173°—that is, 33° as shown on the scale plus the removed 140°. This is the measurement that most earlier workers have made, but Fig. 15 above shows very clearly that the IP extends far on the leading side of the peak—so as to suggest a double profile form. If the IP-MP spacing is instead measured from the IP "centroid"—some 6 or 7° earlier—then the resulting interval is very nearly 180°!

But beyond these basically average-emission properties to consider in trying to understand the relationship between the IP and MP, we have seen above that there are also important dynamical connections. First, both the IP and MP share the 43-P_1 modulation, but only when the 'Q' mode is active. Second, the IP peak (including its entire trailing "component") shows strong positive correlation with the leading emission of the MP as well as negative correlation with its trailing region. Given that these MP regions are conal in nature, it is tempting to conclude that the IP is comprised of a pair of conal components. In short, the putative conal regions of the IP have an angular width comparable to that of the MP, and these respective regions behave similarly dynamically—so that their dynamic midpoints are again nearly 180° apart.

By contrast, the PC is an entirely different animal: it is not opposite to the IP. It shows a different type of emission. It exhibits no periodic fluctuations. And it shows no structures that can be regarded as either conal or core-like.

VI. DISCUSSION

The sideband features in pulsar B0943+10 have been central in rehabilitating the rotating subbeam-"carousel" model for the conal emission in pulsars. First seen in a 430-MHz PS discussed in Paper I, they were interpreted as a roughly 37-P_1 periodic amplitude modulation on the drift-induced phase modulation, and their precise frequency offsets helped to resolve the question of aliasing. Our analyses above have revealed a further two instances of B-mode sidelobes in observations spanning more than 18 hours. Clearly, such tertiary modulation features, although remarkably rare, exhibit highly consistent characteristics. We can then conclude with certainty that these sideband features indicate a physically significant periodicity, which within the subbeam-carousel model corresponds to the circulation time $\hat{P}_3$.

This interpretation was supported in Paper II by a low frequency modulation feature having a periodicity compatible with $\hat{P}_3$. A further low frequency feature of similar periodicity was also identified in a Q-mode PS in Paper IV.

That evidence of a tertiary modulation is now seen to occur in both the Q and B modes—and indeed at several different evolutionary stages of the latter—is consistent with a rotating-carousel subbeam system that has two discrete states: either the 'beamlet' configuration can be sufficiently disordered so that no primary ("drift") modulation is observed, or it is comprised of just 20 evenly spaced beamlets.

The subbeam carousel, however, is not the only extant model for B0943+10's remarkable subpulse-drift phenomena. There are two papers, Clemens & Rosen (2004) and Rosen & Clemens (2008), that explored a non-radial oscillation model and then assessed whether it can produce the specific observations of Paper I. In two papers, Clemens & Rosen (2004) and Rosen & Clemens (2008), their authors first explore a non-radial oscillation model and then assess whether it can produce the specific observations of Paper I. They reanalysed the 430-MHz PS of Paper I, confirmed these earlier results, and reiterated that the sideband feature occurs only within a small section of the full 18-min observation. They then suggest that the sidebands might be produced by a "stochastic variation in pulse amplitudes," but clarify that if periodic amplitude modulation occurs within the drifting-subpulse sequences, then this would favor the carousel as opposed to the non-radial oscillation model. Above, we find three very similar instances of the tertiary amplitude modulation as well as several further instances in which the low frequency periodicity is primary. That these various instances are compatible with each other, exhibit orderly and very long secular variations and show complete frequency independence—these various circumstances would seem to favor the carousel model for drifting subpulses very strongly.

We also report the discovery of a bright precursor component in the Q mode of pulsar B0943+10, falling some 50° longitude prior to the star's MP. This PC is almost fully linearly polarized with a nearly constant PPA traverse. Further, its constituent radiation is "spiky" in character, as opposed to being comprised of broad subpulses—in this respect similar to that seen in pulsar B0656+14 (*e.g.*, Weltevrede *et al* 2006b). Some residual PC emission is also seen in the B mode at a very low level and at a PPA orthogonal to that of the Q mode. In short, this PC feature does not appear to be either conal or corelike.

These curious properties prompted us to compare B0943+10's modal emission characteristics with an ostensibly similar star, B1822–09, as it also exhibits two modes (also denoted B and Q) and a highly linearly polarized PC in one of its modes. These pulsars have similar properties in terms of period, magnetic field, spindown energy and age. However, their inferred emission geometries are very different: B0943+10 has a small magnetic inclination angle and a highly tangential sightline traverse; whereas we argue above that B1822–09 has a nearly orthogonal magnetic geometry and that our sightline traverses its emission cone centrally. Both stars have MP emission characteristics, both in terms of quantitative geometry and dynamics, that are fully comprehensible in terms a core-cone polar cap emission model. In this context, we find that the PC emission is aberrant: not only are its characteristics neither conal nor core-like, but the PC's positions within the profiles of these two stars with well identified polar-cap emission regions would seem to rule out any similar origin.

The fractional linear polarization in most pulsar profiles tends to be low—or at least far from complete. However, the PC emission in both of these stars is nearly 100% linearly polarized. Generally single pulses can be highly polarised (*e.g.*, Mitra *et al* 2009), but a number of depolarizing effects usually lead to substantial profile depolarisation. Recently Johnston & Weisberg (2006) have pointed out that young pulsars with higher spindown energies tend to show relatively simple and highly polarised average profiles. They hypothesize a possible time evolution for pulse profiles suggesting that high $\dot{E}$ pulsars have relatively simple profiles that arise from a single cone of emission high in the magnetosphere. In turn, the depolarization effects are less effective at larger heights, and thus the profiles retain their polarization over a wide range of frequencies. This behavior seems compatible with B1822–09's PC polarization properties: it remains highly polarized from below 243 MHz (Gould & Lyne 1998) to 3.1 GHz (Johnston *et al* 2008).

Following this line of argument, the PC—because it is emitted at high altitude—will proceed the MP. No surprise. However, little more can be said; we thus far have little specific idea just where the PC arises. The PC location is far from the MP, where the RVM predicted PPA is generally flat, as also seen in our observations. However the full PPA traverse in these pulsars are not fully revealed, hence to see the effect of aberration/retardation at the PC location is difficult. We note also that Petrova (2008a,b) has attempted to understand B1822–09's IP, PC and MP emission in terms of scattering effects within the pulsar magnetosphere.

We now turn our attention to the emission-reversal model proposed by Dyks *et al* (2005) to explain the anti-correlation between the intensity of the PC and the IP in B1822–09. They proposed that the PC and the IP are emitted from the same source which reverses emission direction during the different modes. In their model, B1822–09 has a nearly orthogonal geometry (in agreement with our findings). The physical source of the IP & PC is located on the same pole as the MP, and the apparent IP results from inwardly directed emission from the source of the PC. This resolves the problem of information transfer between the poles: if the IP and the PC are emitted from opposite poles, how can their behavior be so strongly anti-correlated?

However, we find that the MP and the IP are similar in their polarization properties and experience the same strong modulation in the 'Q' mode. As argued above, they are both compatible with core-cone emission in the polar-cap model. We also find that the IP and MP are separated by almost exactly 180°, not 186° as found in Dyks *et al* (2005). The PC is markedly different, suggesting a physically different origin from the other two components. This indicates that the MP and IP are both outwardly emitted and are produced by similar processes above the respective two magnetic poles.

Another possibility for the emission reversal model is that the source of the IP and PC is located on the opposite pole from the MP and that the IP is outwardly emitted, whereas the PC is inwardly emitted. Propagation through the closed magnetosphere could explain the unique characteristics of the PC emission, and the MP-IP similarities are easily explained in this model, but the question of information transfer between the poles arises again: the MP behavior is regulated by the same modes as the PC and IP.

These various objections do not completely refute the Dyks *etal* model; they merely pose some problems for their current application to B1822–09, and these problems may be readily explicable under the emission-switching paradigm.

The discovery of a PC in B0943+10 which is so similar to the well-known PC of B1822–09 shows that such a component is not unique, and explaining its origins could have important ramifactions for our understanding of pulsar physics. We should expect that there is one underlying physical process which regulates the modes and therefore the appearance of such divers phenomena as subpulse drifting, polarization characterstics, pulse-shape dynamics, and the presence of a PC. While the similarities between two stars are certainly telling, their dissimilarities are also important for any model purporting to explain the PC in either pulsar. We cannot expect that the alignment of the axes, the sightline traverse β/ρ, or the mode-dependent changes in brightness of the pulsar, play a role in the production of the PC and its modal behavior.

Acknowledgments: We are pleased to acknowledge Jarek Dyks, Janusz Gil, Svetlana Suleymanova and Geoffrey Wright for their critical readings of the manuscript. One of us (JMR) thanks the Anton Pannekoek Astronomical Institute for their generous hospitality and the NWO and ASTON for their Visitor Grant. Portions of this work were carried out with support from US National Science Foundation Grants AST 99-87654 and 08-07691. Arecibo Observatory is operated by Cornell University under contract to the US NSF. This work used the NASA ADS system.

REFERENCES

Alpar, M. A., Guseinov, O. H., Kiziloğlu, Ü., & Öegelman, H. 1995 A&A, 297, 470
Asgekar, A. A., & Deshpande, A. A. 2001, M.N.R.A.S., 326, 1249 (Paper II)
Clemens, J. C., & Rosen, R. 2004, Ap.J., 609, 340
Deshpande, A. A., & Rankin, J. M. 1999, Ap.J., 524, 1008
Deshpande, A. A., & Rankin, J. M. 2001, M.N.R.A.S., 322, 438 (Paper I)
Dyks, J., Zhang, B., & Gil, J. 2005, Ap.J., 626, 45
Dyks, J., Frackowiak, M., Slowikowska, A., Rudak, B., & Zhang, B. 2006, *Ch. J. Astr.&Astrop.*, 6, 85
Fowler, L. A., Morris, D., & Wright, G.A.E. 1981, A&A, 93, 54
Fowler, & Wright, G.A.E. 1982, A&A, 109, 279
Gil, J. A., Jessner, A., Kijak, J., Kramer, M., Malofeev, V., Malov, I., Seiradakis, J. H., Sieber, W., & Wielebinski, R. 1994, A&A, 282, 45
Gould, D.M., & Lyne, A.G. 1998, M.N.R.A.S., 301, 253.
Johnston, S., & Weisberg, J. M. 2006, M.N.R.A.S., 368, 1856
Johnston, S., Karastergiou, A., Mitra, D., & Gupta, Y., 2008, M.N.R.A.S., 388, 261
Mitra, D., Gil, J. & Melikidze, G. I., 2009, Ap.J. Lett., 696, 141
Petrova, S. A. 2008a, M.N.R.A.S., 384, L1
Petrova, S. A. 2008b, Ap.J., 673, 400
Mitra, D., Rankin, J. M. & Gupta, Y. 2007, M.N.R.A.S., 379, 932
Rankin, J. M. 1993, Ap.J., 405, 285 and A&A Suppl., 85, 145 (ETVI)
Rankin, J. M., & Ramachandran, R. 2003, Ap.J., 590, 411
Rankin J. M., Suleymanova, S. A., & Deshpande A. A. 2003, M.N.R.A.S., 340, 1076 (Paper III)
Rankin J. M., & Suleymanova, S. A. 2006, A&A, 453, 679 (Paper IV)
Rosen, R., & Clemens, J. C. 2008, Ap.J., 680, 671
Ruderman, M. A., & Sutherland, P. G. 1975, Ap.J., 196, 51
Suleymanova S. A., Izvekova V. A., 1984, Sov. Astron. 28, 53
Suleymanova, S. A., Izvekova, V. A., Rankin, J. M., & Rathnasree, N. 1998, *J. Astr.&Astron.*, 19, 1. (SIRR)
Suleymanova, S. A., & Rankin, J. M. 2009, M.N.R.A.S., 396, 870 (Paper V)
Weltevrede, P., Edwards, R. T., & Stappers, B. J. 2006a, A&A, 445, 243
Weltevrede, P., Wright, G.A.E., Stappers, B. J., & Rankin, J. M. 2006b, A&A, 458, 269
Weltevrede, P., Stappers, B. J., & Edwards, R. T. 2007, A&A, 469, 607
Zhang, B., Sanwal, D., & Pavlov, G. 2005, Ap.J., 624, 109